Int. J. Electrochem. Sci., 7 **(2012)** 8794 - 8812

International Journal of
ELECTROCHEMICAL
SCIENCE
www.electrochemsci.org

Electro-Oxidation of Benzyl and Aliphatic Alcohols on *polyNiTSPc*- and $Ni(OH)_2$-Modified Glassy-Carbon and Gold Electrodes

María Soledad Ureta-Zañartu[1,*], *Thaís González*[1], *Francisco Fernández*[1], *Daniela Báez*[1],
Cristhian Berríos[1], *Claudio Gutiérrez*[2]

[1] Departamento de Ciencias del Ambiente, Facultad de Química y Biología, Universidad de Santiago de Chile, C. Libertador Bernardo O'Higgins 3363, Estación Central, Santiago, Chile.
[2] Instituto de Química Física "Rocasolano", CSIC, C. Serrano, 119, 28006-Madrid, Spain
[*]E-mail: soledad.ureta@usach.cl

Received: 20 July 2012 / *Accepted:* 21 August 2012 / *Published:* 1 September 2012

The electrooxidation in a pH 11 carbonate/hydrogen carbonate buffer electrolyte of benzyl alcohol (BA) and several primary and secondary aliphatic alcohols on *polyNiTSPc*- and $Ni(OH)_2$-modified glassy-carbon (GC) and gold electrodes was studied by cyclic voltammetry (CV) and with an electrochemical quartz crystal microbalance (EQCM). The films were formed by repetitive cyclic voltammetry in Ni(II)tetrasulphophthalocyanine (NiTSPc) and nickel(II) nitrate solutions, respectively. Although previous *XPS* results indicated a very similar environment for the Ni(II) ion in *polyNiTSPc* and $Ni(OH)_2$ electrodeposited films, their electrochemical behaviour is different, which is probably associated with the hydrophobic-hydrophilic character of the film. The aliphatic alcohols are oxidized on both *polyNiTSPc*/GC and $Ni(OH)_2$/GC, whereas BA is oxidized only on the former. Probably the high hydration of $Ni(OH)_2$ prevents the expulsion of water from the interface required for the oxidation of BA. On *polyNiTSPc*/Au/Q the oxidation of BA takes place exclusively, and with high efficiency, on the Au substrate. We attribute this lack of activity of Ni(III) in *polyNiTSPc*/Au/Q to the high activity of the gold substrate, which depletes the concentration of BA to such an extent as to preclude its reaction with Ni(III). The oxidation of primary and secondary aliphatic alcohols on *polyNiTSPc/Au/Q* also occurs at the gold surface only, although the current is higher in the presence of the film.

Keywords: benzyl alcohol electro-oxidation; aliphatic alcohols electrooxidation; *polyNiTSPc*-modified electrodes; $Ni(OH)_2$-modified electrodes; *EQCM*

1. INTRODUCTION

When in acidic media alcohols are electrooxidized on noble metals these become poisoned by CO [1], which has led to the search for other metals. Other approach has been to use alkaline media, in which all the works mentioned in this introduction were carried out. Sprague et al. [2], using a numerical model, concluded that the oxidation of ethanol proceeds better in an alkaline electrolyte. Recently, Xie et al. [3] concluded that for methanol Pt was more active than Pd, and that primary alcohols gave higher currents than branched ones with the same number of carbon atoms. Santasalo-Aarnio [4] found that Pd works better in alkaline media, but is poisoned by CO. We have recently reported [5] that on gold aromatic alcohols are more easily oxidized than aliphatic alcohols, which was attributed to the hydrophobic character of the former, which displaced water molecules from the electrode surface, leaving it more accessible to the reactant. An interesting study [6] with isotope labelling and sum-frequency generation of ethanol electrooxidation on Pt reported that in alkaline media C-C bond cleavage and CO formation occur as early as 0.05 V *versus* RHE, and that CO is oxidized at ≈0.45 V, a potential 0.2 V lower than that in acidic media.

It has been postulated that the oxidation of alcohols on Ni electrodes is mediated by Ni(III) in a Ni oxy-hydroxide, which would act as a mediator, a chemical reaction between the organic compound and Ni(III) being immediately followed by the reoxidation of Ni(II) in a catalytic cycle [7,8]. Nickel-based compounds have been used recently as modifiers of noble metals electrodes for use in fuels cells [9]. Thus, Qi et al. and Miao et al. [10,11] used nickel-palladium alloy and nanoparticles as electro-catalysts in the oxidation of methanol and ethanol. Motheo et al. [12] found that the electro-oxidation of benzyl alcohol on a Ni electrode in 0.01 M NaOH yields benzoic acid and benzaldehyde, the peak potential being 0.3 V more positive than that of Ni(II) oxidation, which implies that no chemical reaction between Ni(III) and the alcohol is occurring.

Electrodes coated with electrodeposited films of nickel complexes, typically phthalocyanines and porphyrins, continue to be actively investigated [13]. When the film is formed from aqueous Ni(II) species (i.e. Ni(II) tetrasulphophthalocyanine, *NiTSPc*) its electrochemical behavior in alkaline medium is very similar to that of nickel hydroxide films, a stable CV being obtained after a few potential cycles in 0.1 M NaOH [7,8,14]. The attachment of the Ni(II)TSPc to the electrode surface via an oxygen bridge, M–O–Ni(II), is a possibility [14]. Electrodeposited *polyNiTSPc* films are useful for the electrooxidation of organic compounds [15-17]. Previous work has shown that in a pH 11 buffer ethylene glycol is oxidized at both gold and Ni(III) sites of *polyNiTSPc*/Au electrodes, whereas methanol is basically not [16]. Trevin et al. [18] found that on *GC* modified with films of Ni(II) tetrasulpho- and tetraamino-phenyl porphyrin and poly-Ni*salen*, ethanol oxidation in 0.1 M NaOH produced in both the positive and negative sweeps an anodic peak at a potential 0.2 V more positive than that of Ni(II) oxidation. With increasing alcohol concentration the peak current of ethanol oxidation saturated in a Langmuir-like way at a few mM concentration. On the contrary, early studies of alcohols oxidation at electrodes modified with polymeric film of Ni(II) macrocycles reported that the peak currents were proportional to the alcohol concentration, even up to a 0.4 M concentration [12,19-20].

We are still far from knowing why the electrodes modified with films of Ni(II)-complexes are more active than those of $Ni(OH)_2$ for the electrooxidation of organic compounds. Here we have studied the electrooxidation of several alcohols on gold and glassy carbon electrodes modified with *polyNiTSPc* and $Ni(OH)_2$ films, in order to elucidate the role of the substrate and of the structure of the Ni(II) film in the electrooxidation process. We included benzyl alcohol in the study because we expected a π-π interaction between its aromatic ring and the phthalocyanine ligand, which should lead to an increased electrochemical activity as compared with that for aliphatic alcohols.

2. EXPERIMENTAL

Benzyl alcohol (*BA*), ethanol, ethylene glycol, NaOH, $NaHCO_3$, Na_2CO_3 and $Ni(NO_3)_2$, all of them p.a. from Merck, 1- and 2-propanol and Ni(II)*TSPc* from Aldrich were used as received. The solutions were freshly prepared with deionized, twice-distilled water and deaerated with N_2. A pH 11 carbonate/hydrogen carbonate buffer was the usual support electrolyte, although in some experiments 0.1 M NaOH was used. Usually the electrode was introduced in the alcohol solution at open circuit, unless otherwise specified.

SEM images of gold-coated stabilized *polyNiTSPc* and $Ni(OH)_2$ films, the former on both GC-DD and on Au-D, and the latter on GC-SP, were collected with a Scan Electron Microscopy LEICA S 440 instrument which allows to determine chemical composition by Energy Dispersive Spectroscopy (EDS).

2.1 Electrode preparation

Several types of electrode were used: a 3 mm-diameter glassy-carbon disc (GC-D) from CH Instruments, a detachable 14 mm-diameter glassy carbon disc (GC-DD) from Carbone Lorraine, a 3.5 mm-diameter screen-printed glassy-carbon (GC-SP) from DropSens, a 2 mm-diameter gold disc (Au-D) from CH Instruments, and a 10-MHz Au-covered *AT*-cut quartz electrode (Au/Q) from Elchema, with a geometric area of 0.25 cm^2, a resonant area of 0.24 cm^2 and a constant of 4.4 ng Hz^{-1} cm^{-2}. The Au-D and GC-D disc electrodes were polished with 0.1 μm alumina powder and sonicated for 10 min. GC-SP and Au/Q electrodes were cleaned with distilled water and its cleanness checked by CV in 0.5 M H_2SO_4. A Pt helix of high area was the counter electrode, and a KCl-saturated Ag/AgCl electrode, connected to the cell by a Luggin capillary, was the reference.

Films of *polyNiTSPc* were prepared as previously described [16], by 15 (in the case of Au/Q for EQCM) and 20 (in the case of GC-D, GC-DD and Au-D) repetitive cyclic voltammograms (RCVs) at 0.01 V s^{-1} in 0.1 M NaOH containing 1 mM NiTSPc, after which the electrode was rinsed with water, introduced in the pH 11 buffer electrolyte and stabilized by 5 RCVs at 0.1 V s^{-1}. The deposited mass was of the order of 5.9 μg cm^{-2}, which corresponds to a thickness of about 36 nm (apparent density 1.6 g cm^{-3}) [16]. The $Ni(OH)_2$ films were obtained with 5 RCVs between -0.4 and 1.1 V in a $Ni(NO_3)_2$ solution of pH 7.3 [21,22] and stabilized by 5 RCVs at 0.1 V s^{-1} in 0.1 M NaOH. The net mass increase due to the $Ni(OH)_2$ film formation was about 5 μg cm^{-2}.

SEM images were collected with a Scan Electron Microscopy LEICA S 440 instrument, which allows to determine chemical composition by Energy Dispersive Spectroscopy (EDS). All the samples were previously coated with gold.

3. RESULTS AND DISCUSSION

3.1. Characterization of the electrodes

3.1.1. Determination of film thickness.

The amount of *polyNiTSPc* or $Ni(OH)_2$ deposited at the electrode cannot be determined from the charge under the Ni(II) oxidation peak in a *CV*, since the peak current is not proportional to the scan rate (plots of log j_p *vs.* log (*scan rate*) always have a slope considerable smaller than one), *i.e.*, the charge under the peak decreases with increasing scan rate. This has been associated with a diffusional control of charge transport through the film, due to the entry/exit of ions necessary to maintain electroneutrality [8]. Previous work has shown that both the cumulative mass and the anodic peak current density of Ni(II) oxidation increase linearly with the number of deposition cycles, which led us to define the Peak Current Density (*PCD*) parameter obtained from *CV*s at 20 mV s^{-1} as a measure of the relative thickness of the *polyNiTSPc* films [8]

The $Ni(OH)_2$ films did not show the typical behavior of surface processes either. The value of dlog(j_p)/dlog(v) was about 0.7, depending on the film thickness. Yang [23] reported that the density of $Ni(OH)_2$ obtained by chemical precipitation varies between 1.7 and 2.6 g cm^{-3}, with a Ni content of about 50-59 wt%. Then, deposits of about 5 µg cm^{-2} should be 19.2 - 29.4 nm thick, about 4.1-4.9 mC cm^{-2} being required for oxidizing all the Ni(II) in the film, in fair agreement with the charge of 7.1 mC cm^{-2} found in CVs at 0.1 V s^{-1}.

In summary, the *PCD* parameter is useful for comparing relative thicknesses. In the present work the *PCD* parameter was evaluated from *CV*s at 0.1 V s^{-1} because most scans were recorded at that rate.

3.1.2. SEM and ex-situ AFM microscopy

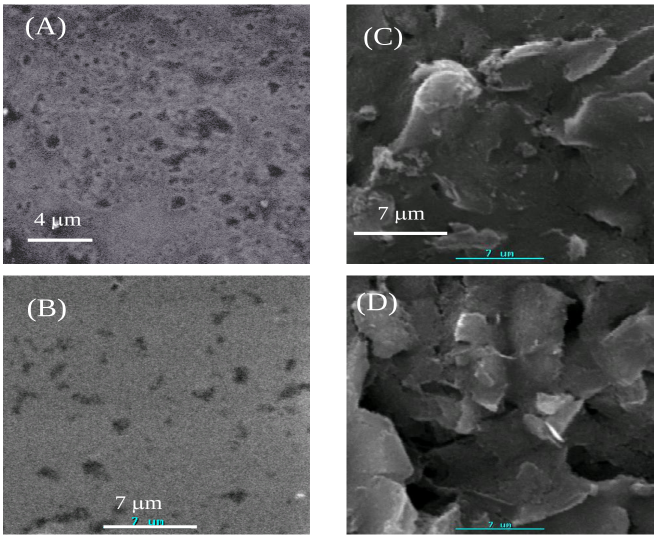

Figure 1. SEM images of stabilized *polyNiTSPc* coatings at: (A) GC-DD; (B) Au-D; (C) $Ni(OH)_2$/GC-SP. (D) corresponds to bare GC-SP.

Figure 1 shows the SEM images of *polyNiTSPc*/GC-DD (A), *polyNiTSPc*/Au/Q (B), $Ni(OH)_2$/GC-SP (C), and GC-SP (D). The *polyNiTSPc* films at both GC-DD and Au/Q are similar, showing a uniform coating with craters that reveal a high porosity, whereas in $Ni(OH)_2$/GC-SP films (Fig. 1C) the $Ni(OH)_2$ appears as grains a few nm in diameter scattered over the scaly GC-SP substrate (Fig. 1D).

The EDS spectra of $Ni(OH)_2$/GC-SP (A) and *polyNiTSPc*/Au/Q (B) are shown in Figure 2. The Ni peak is well defined in the nickel hydroxide film (Fig.2A), while it is nearly absent in the *polyNiTSPc* film (Fig. 2B).

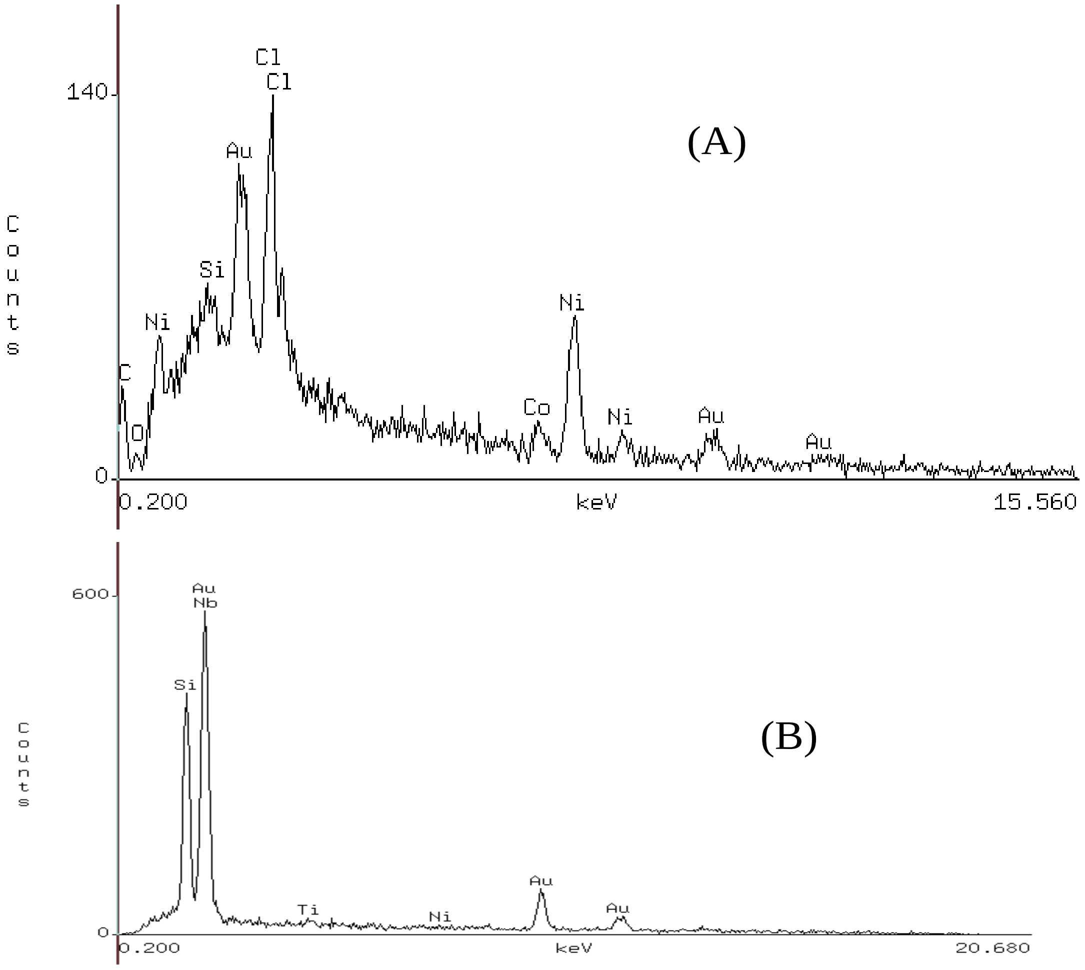

Figure 2. Energy-dispersive X-ray analysis of stabilized coatings of: (A) $Ni(OH)_2$/GC-SP; (B) *polyNiTSPc*/GC-DD

The AFM images of Au/Q electrodes coated with a NiTSPc film (Figure 3) show two types of film, one amorphous (Fig. 3B) and the other made up of closely packed spheres about 0.2-0.3 μm in diameter (Fig. 3C), in agreement with previous reports [24]. Ageing of the film by RCV at 0.01 V s^{-1} in 0.1 M NaOH decreases the regions with spheres.

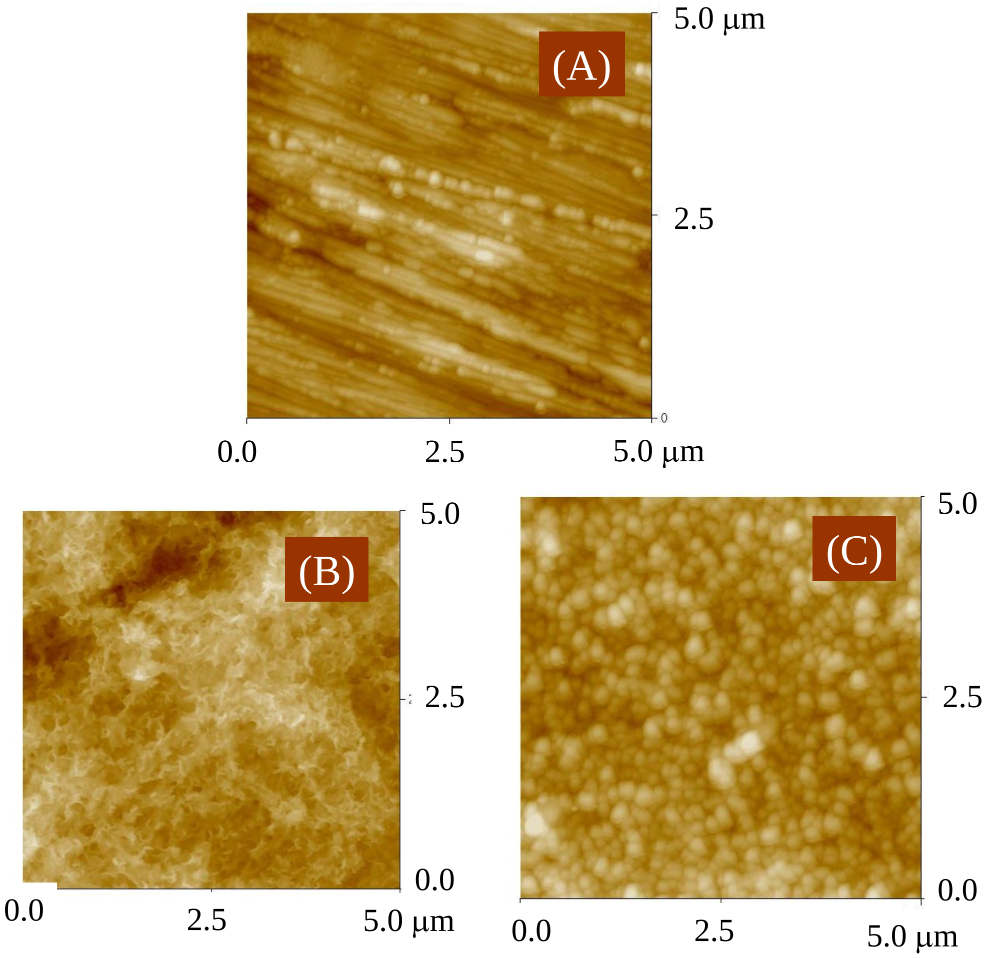

Figure 3. AFM images of: (A) Bare Au/Q. (B) Homogeneous region, and (C) region of closely packed spheres, of Au/Q electrode coated with a *polyNiTSPc* film.

3.1.3. Cyclic voltammetry (CV) and mass changes of the Ni(III)/Ni(II) process

The *CV*s in the pH 11 buffer of *polyNiTSPc* and of $Ni(OH)_2$, both with *GC-D* as substrate, are shown in Figs. 4A and 4B, respectively, and those with Au/Q as substrate in Figs. 4C and 4D, respectively. In all cases there appear in the CV an anodic (A1) and a cathodic (C1) peak corresponding to the non-Nernstian Ni(III)/Ni(II) process. The substrate dramatically affects the CV of the process, as can be seen in Table 1: the anodic and cathodic peak potentials are practically the same, 0.84 and 0.63 V, respectively, for the two films on GC. In contrast, on Au the peak potentials were about 70-150 mV lower: they were 0.74 and 0.51 V for the anodic and cathodic peaks, respectively, also irrespective of the nature of the films. The peak separation, that is, the reversibility of the process, also depended significantly on the substrate, it being about 0.20 V and 0.13 V for the GC and the Au substrates, respectively. The half-sum potential, which is related to the reversible reduction potential of the process, depended also on the nature of the substrate: it was 0.77 and 0.71 V for *polyNiTSPc* and for $Ni(OH)_2$, respectively, on GC, and 0.65 and 0.61 V, respectively, on Au.

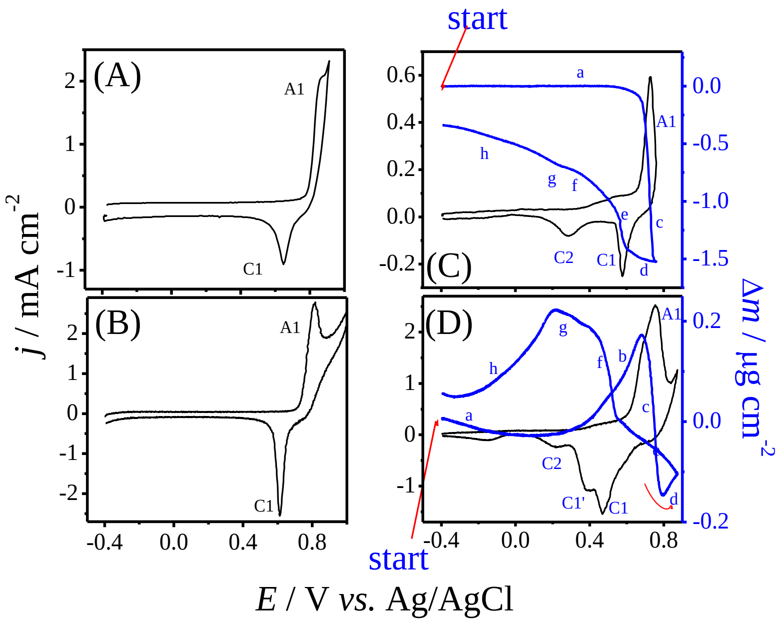

Figure 4. Cyclic voltammograms at 0.1 V s^{-1} in pH 11 buffer electrolyte of a stabilized GC-D electrode coated with a film of: (A) *polyNiTSPc*; (B) $Ni(OH)_2$. (C) and (D) are the CVs of an Au/Q electrode modified with *polyNiTSPc* and $Ni(OH)_2$ films, respectively (black curves, left axis) and the simultaneously obtained mass curves (blue curves, right axis).

However, it can be noticed that the nature of the film also played a role in the half-sum potential, since for both substrates that of *polyNiTSPc* was about 60-40 mV higher than that of $Ni(OH)_2$. This points to a slightly different environment of the Ni ions in the two films, as was to be expected. This dramatic influence of the substrate is in agreement with the results of Weng et al. [27] for α-$Ni(OH)_2$ prepared by electrochemical precipitation from nitrate baths (the procedure used in this work): the peak separation of the Ni(III)/Ni(II) process was 0.17 V for α-$Ni(OH)_2$/Pt and higher than 0.34 V for α-$Ni(OH)_2$/Pt/Ti.

The presence of peak C2 of gold oxide reduction in the *CV*s of both *polyNiTSPc*/Au/*Q* and of $Ni(OH)_2$/Au/*Q* indicates that both films are porous, as already reported [24], the *polyNiTSPc* films being slightly more so. The reduction of the gold oxide is slightly inhibited (by 20 mV only) by both *polyNiTSPc* and $Ni(OH)_2$ films.

Table 1. PCD and peak potentials obtained from the cyclic voltammograms in the *pH* 11 buffer electrolyte of *polyNiTSPc* and $Ni(OH)_2$ films deposited on *GC-D* and *Au/Q* electrodes. Data obtained from the CVs in Fig. 4.

	polyNiTSPc/GC-D	polyNiTSPc/Au/Q	$Ni(OH)_2$/GC-D	$Ni(OH)_2$/Au/Q
PCD/mA cm^{-2}	2.05	0.59	2.71	2.47
Ep_{A1} /V	0.86	0.73	0.82	0.75
Ep_{C1} /V	0.65	0.58	0.62	0.47& 0.39

The mass curves of *polyNiTSPc*/Au/*Q* and Ni(OH)$_2$/Au/*Q* electrodes (Fig. 4C and 4D) have been described [9,17], and also under the same experimental conditions of this work [5]. For the stabilized *polyNiTSPc*/Au/*Q* electrode (Fig. 4C) the mass remains almost constant during most of the positive scan (region *a*), which unequivocally shows that already at the start potential most of the water has been expelled from the Au surface. The mass constancy in the region of gold oxidation is possibly due to a positive shift of gold oxidation by the *polyNiTSPc* film, the mass increase being then compensated by the beginning of the mass decrease due to Ni(II) oxidation. On the contrary, with Ni(OH)$_2$/Au/Q the mass increases from 0.4 V until Ni(II) oxidation starts (regions *a* and *b* in Fig. 4D).

In both films a mass decrease attends the oxidation of Ni(II), this mass decrease (region *c*) being much larger for *polyNiTSPc* than for Ni(OH)$_2$ (Figs. 4C and 4D, respectively), although the *PCD*s, and therefore the amount of active Ni, is higher for Ni(OH)$_2$/Au/Q. This dramatic difference in the mass curves shows that *ECQM* is a good adjunct to conventional electrochemical techniques, because the very large mass decrease attending Ni(II) oxidation in the *polyNiTSPc* film supports that in the latter a hydrophobic environment around the Ni(II) ions favours the expulsion of water.

Two different slopes appear during the mass increase due to Ni(III) reduction in Ni(OH)$_2$/Au/Q (regions *e* and *f*), pointing, as discussed below, to two different structures of the Ni(OH)$_2$ film, in agreement with the shoulder C1' in the reduction peak in the *CV*. The mass increases slightly during gold oxide reduction (region *g*), most probably due to an adsorption of water and/or ions on the pristine Au surface that overcompensates the loss of oxygen, and afterwards decreases to a final mass higher than the initial one. On the contrary, with the *polyNiTSPc*/Au/Q electrode, in the negative sweep the mass increases smoothly to a value lower than the initial one.

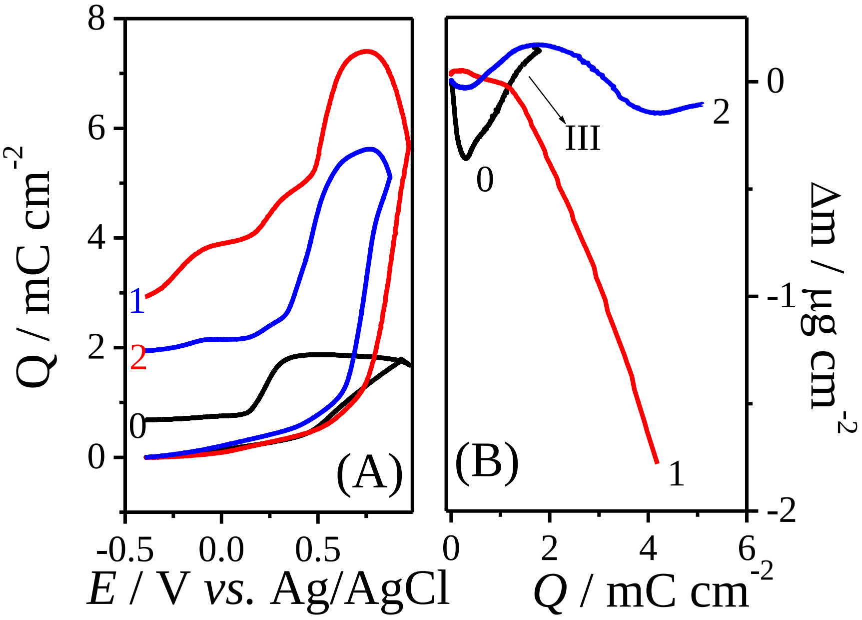

Figure 5. (A) Charge density (Q) as a function of the potential and (B) Mass change (Δm) as a function of the charge density, for Au/Q (0), *polyNiTSPc*/Au/Q (1) and Ni(OH)$_2$/Au/Q (2) electrodes in pH 11 buffer electrolyte. Data obtained from the CVs in Fig. 4.

The cumulative charge in the CVs at 0.1 V s^{-1} in pH 11 buffer in Figs. 4C and 4D is plotted in Figure 5A for Au/Q (black curve 0), *polyNiTSPc*/Au/Q (red curve 1) and $Ni(OH)_2$/Au/Q (blue curve 2) electrodes. For both modified electrodes the charge continues increasing after potential reversal, which shows that the films shift positively the formation of gold oxide.

Mass change *vs*. charge plots during the positive sweep are given in Fig. 5B. The slope for bare gold-quartz in the region of gold oxide formation is 0.33 mg C^{-1} (region III in curve 0), which is 4.0 times higher than that of 0.083 mg C^{-1} corresponding to the formation of a monolayer of AuO. This evidences that water and/or anions adsorb on the gold oxide. In this plot it becomes more readily apparent that the mass decrease attending Ni(II) oxidation is much larger for *polyNiTSPc* than for $Ni(OH)_2$ (curves 1 and 2, respectively).

As is well known, nickel hydroxide can have two different structures, α- and β-$Ni(OH)_2$, with higher and lower hydration, respectively [9,22,25]. α-$Ni(OH)_2$ is very disorganized, with an inter-slab distance of 8 Å, whereas β-$Ni(OH)_2$ is more structured, this distance being only 4.6 Å [22]. The oxidation of Ni(II) in electrochemically precipitated $Ni(OH)_2$ involves a mass increase and decrease, respectively, for α-$Ni(OH)_2$ and β-$Ni(OH)_2$, the latter having been obtained by *RCV* of the former [21,26]. The same behaviour has been found here in the stabilization by five *CV*s of the $Ni(OH)_2$/Au/Q electrode in 0.1 M NaOH: in the first *CV*, during the Ni(II) oxidation a small mass decrease precedes the mass increase, whereas in the second and successive *CV*s (not shown) the behaviour is the opposite, a small mass increase preceding a small mass decrease. Probably the presence of a shoulder in the Ni(III) reduction peak of the $Ni(OH)_2$/Au/*Q* electrode (peak C1' in Fig. 4D) indicates the presence of some residual α-$Ni(OH)_2$. Unfortunately, we were unable to determine by X-ray diffraction the structure of the film because it was too thin for the available equipment.

In previous work [24] both *polyNiTSPc* and $Ni(OH)_2$ films on *ITO* were characterized by *XPS*. The Ni2p spectra were very similar, which led us to conclude that the Ni(II) in the polymer had a hydroxide-type structure. As for films of polyNi(II)tetrasulphophenyl-porphyrin, which are similar to those of *polyNiTSPc*, the N1s spectrum showed the presence of a N-H bond, probably as a result of the replacement of Ni(II) by hydrogen in the plane of the macrocycle, this being in agreement with the Ni2p spectrum [7].

3.1.4. Electrochemical impedance spectroscopy of Au/D, polyNiTSPc/Au-D, and $Ni(OH)_2$/Au-D electrodes in 0.1 M NaOH

The impedance curves of Au-D and of Au-D coated with *polyNiTSPc*/Au-D and $Ni(OH)_2$ films in 0.1 M NaOH (Figures 6 A to C) were fitted to *Randles*' diagram, as in previous works [5,8,27,28], using the NOVA 1.7 software to fit the semicircle. Au shows the characteristic semicircle (Fig. 6A) only at the positive potential limit, 1.0 V, at which oxygen evolution starts (Fig. 6D). With the *polyNiTSPc*/Au-D electrode the semicircle is first observed at 0.552 V (Fig. 6B), the peak potential of Ni(II) oxidation (Fig. 6E), R_{ct} dramatically decreasing upon a further voltage increase of only 30 mV (Fig. 6B'). Quite unexpectedly, the $Ni(OH)_2$/Au/Q electrode first shows the semicircle at 0.560 V (Fig. 6C), at the minimum between Ni(II) oxidation and oxygen evolution (Fig. 6F), and with an R_{ct} several times higher than that of *polyNiTSPc* at the corresponding minimum, although the *PCD* parameters are very similar (Table 2). At the potential of the minimum preceding O_2 evolution, the charge-transfer resistance (R_{ct}) of the $Ni(OH)_2$ film is 5 times higher than that of the *polyNiTSPc* film.

Table 2. Impedance parameters* in 0.1 M NaOH of bare Au-D, and of Au-D coated with films of *polyNiTSPc* and of $Ni(OH)_2$

Electrode Parameter	Au-D	*polyNiTSPc*/Au-D	$Ni(OH)_2$ /Au-D
Potential	1.0 V	0.552 and 0.582 V	0.560 V
R_s / Ω cm^2	6.0	9.2	9.2
R_{ct} / kΩ cm^2	4.94	2.21 0.21	0.99
C_{dl} / μF cm^{-2}	116	844 868	27

*R_s : uncompensated resistance; R_{ct}: charge transfer resistance; C_{dl}: double layer capacitance evaluated using $\omega_{max} = (R\ C_{dl})^{-1}$.

In summary, although the previous *XPS* results indicated a very similar environment for the Ni(II) ion in *polyNiTSPc* and $Ni(OH)_2$ films, their electrochemical behaviour is different, which is probably associated with the hydrophobic-hydrophilic character of the film. For $Ni(OH)_2$ the Ni(II)/Ni(III) process was proposed long ago by Fleischmann et al. [29] to be:

$$Ni(OH)_2 + OH^- \leftrightarrows NiOOH + H_2O + e^- \qquad (1)$$

this clearly being an oversimplification.

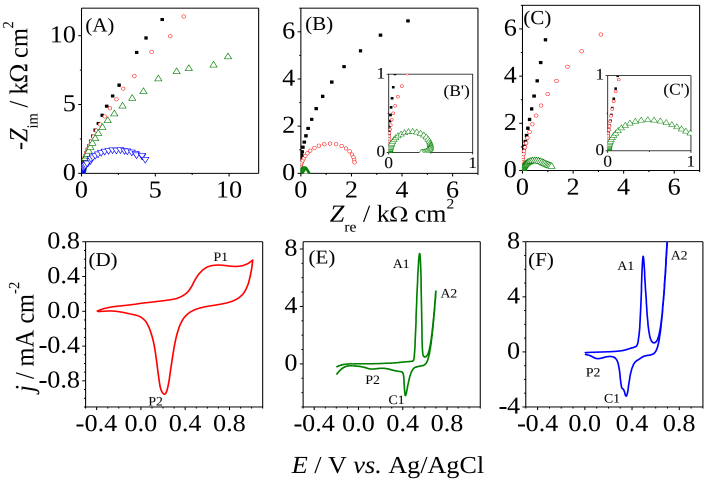

Figure 6. Complex impedance plots in 0.1 M NaOH of: (A) Bare Au-D electrode at 0.4 V (■); 0.6 V (o); 0.8 V (▲) and 1.0 V (▽); (B) *polyNiTSPc*/Au/Q electrode (PCD=7.1 mA cm^{-2}) at 0.522 V (■); 0.552 V (o) and 0.582 V (△) (C) $Ni(OH)_2$/Au electrode (PCD=7.3 mA cm^{-2}) at 0.471 V (■), 0.531 V (o), and 0.560 V (△). D, E and F are the respective CVs at 0.1 V s^{-1}.

The same process would be occurring at *polyNiTSPc* films, for which, in agreement with the XPS results previously reported [15], the nickel would be replaced by hydrogen in the center of the phthalocyanine ring and may form a Ni oxy-hydroxide very similar to $Ni(OH)_2$. Actually the oxidation state of nickel would probably change continuously between two and four over a range of potentials [29]. In any case it is obvious: 1) that the Ni(II)/Ni(III) process involves the transfer of protons and/or hydroxyl ions, 2) that other anions and/or cations are also involved, and 3) that both Ni(II) and Ni(III) are hydrated, which makes for a complex process [9].

The Ni(II)/Ni(III) process shifts negatively with potential cycling, which is attributed to changes in the crystal structure of both $Ni(OH)_2$ and NiOOH [30,31].

3.2 Oxidation of benzyl alcohol and aliphatic alcohols at polyNiTSPc/GC and $Ni(OH)_2$/GC electrodes

3.2.1 Oxidation in the pH 11 buffer of benzyl alcohol at polyNiTSPc and $Ni(OH)_2$ films deposited on GC-D electrodes

Bare GC has no activity for the oxidation of alcohols (not shown). On the contrary, at the *polyNiTSPc/GC-D* electrode the addition of 1 mM BA provoked in the CV at 0.02 V s^{-1} a current increase that extended from the peak potential of Ni(II) oxidation up to the positive potential limit (curve 2 in Fig. 7A), as compared with that in the pH 11 buffer (curve 0). Since the oxidation of BA starts at the peak potential of Ni(II) oxidation, it is probable that it occurs by a chemical reaction between *BA* and Ni(III), as reported for other alcohols [16]. In order to determine the effect of donor and acceptor substituents at position 2 of the benzene ring, the CVs in the presence of 1 mM 2-ClBA and 1 mM 2-methoxy-BA (curves 1 and 3 in Figs. 7A and 7C, respectively, only the positive scans being shown in the latter). As expected, the oxidation of 2-ClBA is more difficult than that of BA, the potential being shifted positively by about 34 mV, while the oxidation of 2-methoxyBA begins at a slightly less positive potential than that of BA, together with the beginning of the oxidation of Ni(II). This is in agreement with previous results at a bare gold electrode [5].

The *CV* at 0.1 V s^{-1} in the pH 11 buffer electrolyte of a $Ni(OH)_2$/*GC-D* electrode (curve 0 in Fig. 7B) is barely affected by the presence of even a very high concentration of BA, 0.2 M (curve 1), because the anodic charge is nearly the same as that in base electrolyte, indicating that $Ni(OH)_2$ shows negligible activity for *BA* oxidation. However, there is a small anodic peak in the negative scan, which shows that there is some chemical reaction between Ni(III) and *BA*. This lack of activity is in agreement with the results of Golikand et al. [32], who found no activity of $Ni(OH)_2$/Ni electrodes for methanol oxidation, while nickel-dimethylglyoxime/Ni electrodes did show some activity.

The remarkable difference between the high activity of the *polyNiTSPc/GC-D* electrode for the oxidation of BA, as compared with the complete lack of activity of the $Ni(OH)_2$/*GC-D* electrode, could be due to the hydrophobic character of the phthalocyanine aromatic ring, which favours the adsorption of the also aromatic BA and the expulsion of water from the interface, while the high hydration of $Ni(OH)_2$ would preclude the adsorption on it of the aromatic BA .

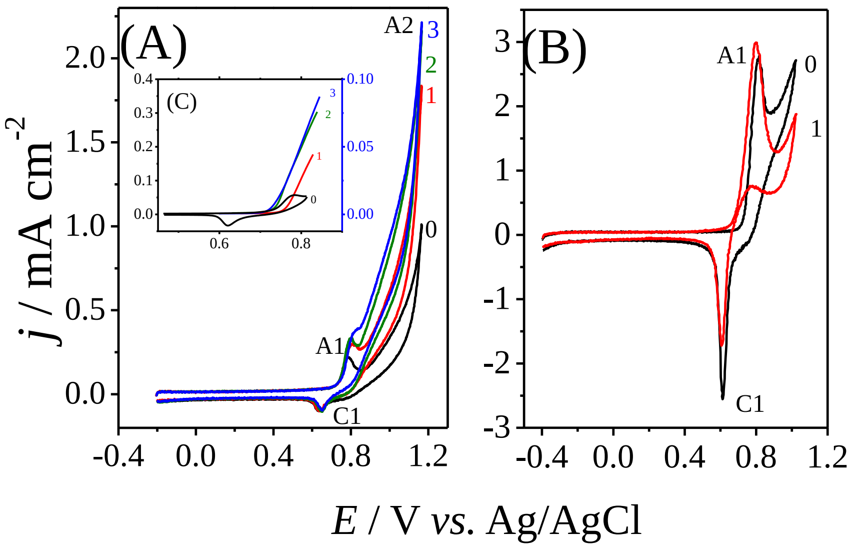

Figure 7. (A): CVs at 0.02 V s^{-1} at *polyNiTSPc*/GC-D in pH 11 buffer (0) and in the presence of 1 mM 2-ClBA (1), 1 mM BA (2) and 1 mM 2-methoxyBA (3). (B): CVs at 0.1 V s^{-1} in pH 11 $Ni(OH)_2$ in buffer electrolyte (0) and in the presence of 0.2 M BA (1). (C) Only the positive scan of (A), except for the CV in base.

3.2.2 Oxidation of aliphatic alcohols on polyNiTSPc and $Ni(OH)_2$ films deposited on GC-D electrodes

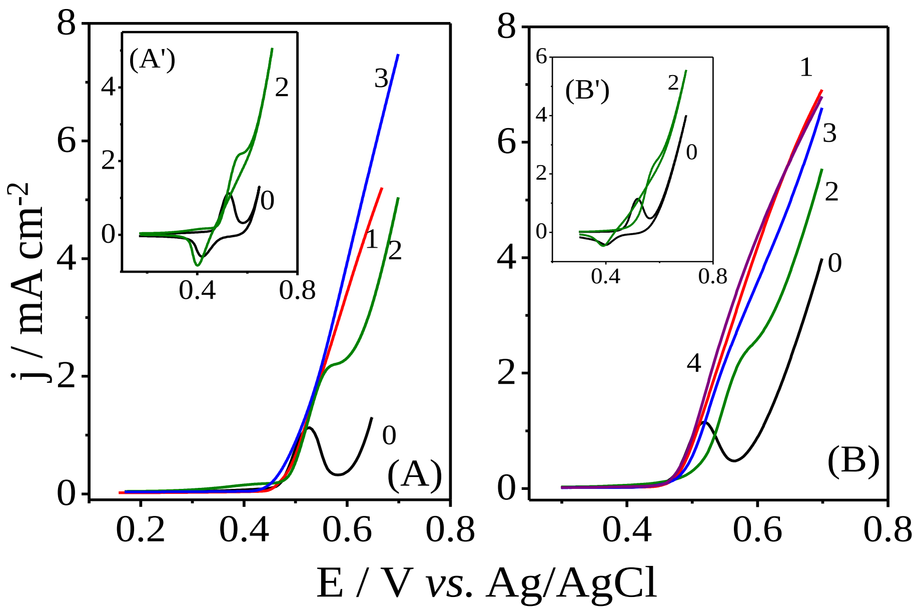

Figure 8. Positive scans at 0.05 V s^{-1} in 0.1 M NaOH (0) and in the presence of 0.5 M 1-propanol (1); 2-propanol (2); 1-butanol (3) and ethylene glycol (4), for *polyNiTSPc*/GC-D (A) and $Ni(OH)_2$/GC-D electrodes (B). The insets are the CVs in base and in 2-propanol.

In 0.1 M NaOH the peak potential of Ni(II) oxidation is the same, 0.52 V, for both films deposited on GC-D (Fig. 8). On both electrodes the oxidation of 1- and 2-propanol, 1-butanol and ethylene glycol (all at a 0.5 M concentration) is mediated by Ni(III), since it starts together with that of Ni(II), as can be seen in the positive scans at 0.05 V s^{-1} for *polyNiTSPc*/GC-D (Fig. 8A) and for $Ni(OH)_2$/GC-D (Fig. 8B). Only on the latter does the oxidation of 2-propanol (green curve 2) start at a slightly higher (by about 35 mV) potential, and on both films the current shows a shoulder at about 0.6 V. Ojani et al. [33] also found, using a carbon electrode modified by Ni(II) incorporated in Y zeolites, that in 0.1 M NaOH the oxidation of methanol started together with that of Ni(II).

Oxidation of primary aliphatic alcohols at Ni/NiOOH electrodes in alkaline medium can yield organic acids [29,34]. With Pd and Pt electrodes both the aldehyde and the acid have been obtained in the oxidation of methanol and ethanol, and acetone for 2-propanol [4]. At Pt electrodes C-C bond breaking of ethanol occurs only in the absence of strongly adsorbing anions [35].

In summary, the aliphatic alcohols are oxidized on both $Ni(OH)_2$/GC-D and *polyNiTSPc*/GC-D, whereas BA is oxidized only on the latter. Probably the high hydration of $Ni(OH)_2$ prevents the expulsion of water from the interface required for the oxidation of BA, as previously reported [5].

3.3 Oxidation of benzyl alcohol and aliphatic alcohols at polyNiTSPc/Au/Q and $Ni(OH)_2$/Au/Q electrodes

In a previous work we reported the electrochemical oxidation of several alcohols at gold electrodes in alkaline media [5]. The same experimental conditions were used here, in order to allow a comparison of the results.

3.3.1 Oxidation of benzyl alcohol at polyNiTSPc/Au/Q and $Ni(OH)_2$/Au/Q electrodes

In alkaline media gold shows a much higher activity for aromatic than for aliphatic alcohols, which has been attributed, firstly, to the high hydrophobicity of the first ones, and, secondly, to the absence of blocking species [5]. *CV*s at 0.1 V s^{-1} and the simultaneously recorded mass curves of a *polyNiTSPc*/Au/Q electrode in a pH 11 buffer electrolyte are shown in Fig. 9, and those of $Ni(OH)_2$/Au/Q in Fig. 10. In the absence of *BA* the *CV* of *polyNiTSPc*/Au/Q (curve 0 in Fig. 9A) shows, in addition to the peaks A1 and C1 of the Ni(II)/Ni(III) process, the characteristic peaks P1 and P2 of surface gold oxidation and reduction, respectively, with high current densities similar to those of bare gold, indicating that the *polyNiTSPc* film is very porous [5,36].

On a *polyNiTSPc*/Au/Q electrode the oxidation of BA takes place exclusively, and with high efficiency, on the Au substrate, as clearly shown by the large P3 and P4 peaks of BA oxidation on the positive and negative sweeps, respectively (Fig. 9A). The peak of Ni(II) oxidation is only slightly increased by *BA* (Fig. 9A, curves 1-5), indicating some activity of Ni(III) for *BA* oxidation. We attribute this lack of activity of Ni(III) to the high activity of the gold substrate, which depletes the concentration of BA to such an extent as to preclude its reaction with Ni(III). Effectively, in experiments at higher BA concentrations (not shown) the current in the region of Ni(II) oxidation increased, since so did the concentration of *BA* in the film.

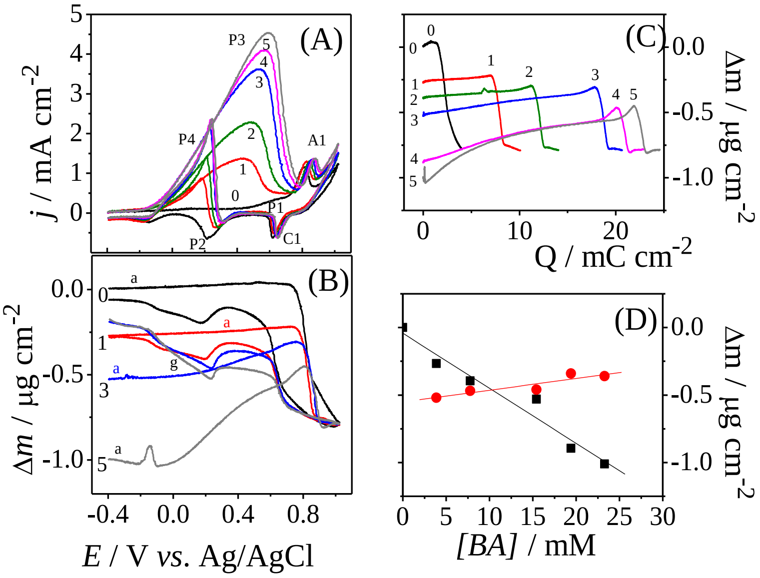

Figure 9. Cyclic voltammograms at 0.1 V s^{-1} (A) and the simultaneously recorded mass curves (B) of *polyNiTSPc*/Au/Q electrode in pH 11 buffer electrolyte (0) and in the presence of: 4.3 mM (1); 8.6 mM (2); 12.9 mM (3); 17.2 mM (4) and 23.3 mM (5) benzyl alcohol. (C): The mass change *vs*. the anodic charge density for curves 0-5 in Figs. 9A and 9B. (D) Mass decrease after one CV (final mass minus initial mass, both at the initial potential) (black squares) and mass decrease attending Ni(II) oxidation (red circles) *vs*. BA concentration.

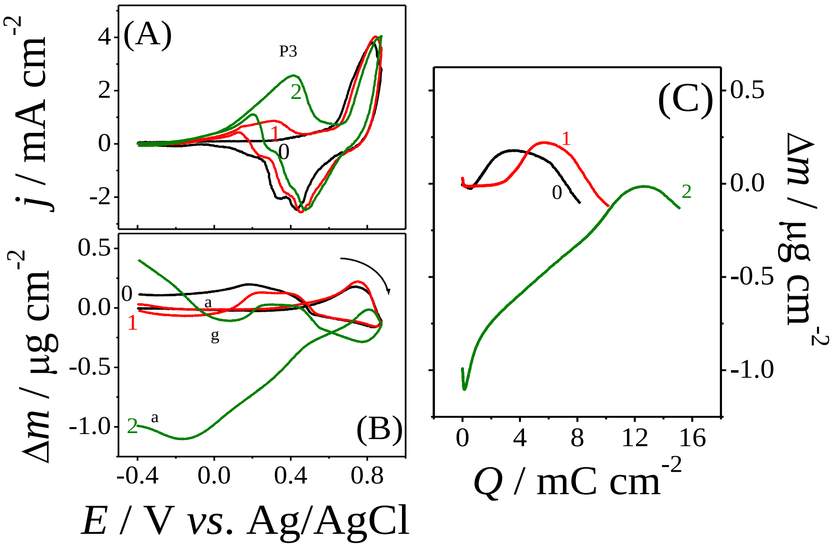

Figure 10. Cyclic voltammograms at 0.1 V s^{-1} (A) and the simultaneously recorded mass curves (B) of $Ni(OH)_2$/Au/Q electrode in pH 11 buffer electrolyte (0) and in the presence of: 8.6 mM (1) and 23.3 mM (2) benzyl alcohol. (C): Mass change *vs*. the anodic charge density for curves 0-2 in Figs. 10A and 10B.

The masses in Figs. 9B and 10B have been made to coincide at the reversal potential (region d in Figs. 4C and D). Similarly to what occurs with bare gold [5], with *polyNiTSPc* the mass at the initial potential decreases monotonically with increasing *BA* concentration (Fig. 9B), this initial mass decreasing linearly with increasing BA concentration (black squares in Fig. 9D). For the same electrode, in the presence of BA the mass increases in the region of peak P3 of *BA* oxidation on the Au substrate (Fig. 9B, curve 2, region *a*), probably because water adsorbs on the sites left free by *BA* oxidation, while in the absence of BA it remained constant (curve 0 in Fig. 9B). The mass increase in the region of peak P4, just after gold oxide reduction (region *g*), increases with increasing *BA* concentration, probably because of a higher adsorption of *BA*, and consequently a higher dehydration of the surface, at these more negative potentials. The higher the *BA* concentration, the more irreversible is the behaviour of the mass, which at the higher *BA* concentrations is much higher at the final than at the initial potential (Fig. 9B) as a consequence of the dehydration of the interphase at the open circuit potential. Note that the mass at the final potential is little affected by the BA concentration, showing the absence of adsorbed residues. This indicates that in the freshly reduced *polyNiTSPc* film more water and/or ions are adsorbed than on the same film held at the initial potential for some time.

The negative $d\Delta m/dQ$ slope in the region of Ni(II) oxidation (nearly vertical segments in Fig. 9C) decreases with increasing *BA* concentration, from -0.53 mg C^{-1} in the absence of *BA* to -0.34 mg C^{-1} in 23.3 mM *BA*. In agreement with this, the mass loss accompanying Ni(II) oxidation decreases linearly with increasing *BA* concentration (red circles in Fig. 9D), pointing again to a higher initial dehydration by *BA*.

The peak currents of *BA* oxidation on the gold substrate on $Ni(OH)_2$/Au/Q (Fig. 10A) were about half those on *polyNiTSPc*/Au/Q (Fig. 9A), the reason for this being that the former film was nearly 4 times thicker, and therefore diffusion of *BA* to Au was more hindered. The peak of Ni(II) oxidation was practically unaffected by the presence of *BA*, which was to be expected, since this was also the behaviour of the $Ni(OH)_2$/*GC-D* electrode (Fig. 7). As in *polyNiTSPc*, the mass at the initial potential decreases with increasing *BA* concentration, and the mass curve becomes the more irreversible the higher the *BA* concentration, so much so that at a 23.3 mM concentration the final mass is 1.4 μg cm^{-2} higher than the initial mass (green curve 3 in Fig. 10B). The mass *vs*. charge plots (Fig. 10C) show changes with the BA concentration similar to those of *polyNiTSPc*/Au/Q (Fig. 9C).

As in the case of bare gold, for both films the current densities of peak P3 of BA oxidation on the Au substrate increase in a Langmuir-like fashion with increasing BA concentration, reaching saturation at about 25 mM BA [5]. The peak current densities are much the same in the absence and presence of the *polyNiTSPc* film, clearly showing that these films, in spite of their very high PCDs, about 7 mA cm^{-2}, are very porous. In the positive sweep the peak potential of BA oxidation on bare gold (peak P3) increases with BA concentration, films of *polyNiTSPc* and $Ni(OH)_2$ shifting the peak potential positively and negatively, respectively, as compared with that for bare gold.

3.3.2 Oxidation of aliphatic alcohols on polyNiTSPc/Au/Q

In the pH 11 buffer the oxidation of several secondary and primary aliphatic alcohols on *polyNiTSPc*/Au/Q also occurs at the gold surface only, as evidenced by the peak P3 in the CVs at 0.01

V s^{-1} for 20 mM 2- and 1-propanol (curve 1 in Figs. 11 A and 11C, respectively) and for 20 mM 2- and 1-butanol (curve 2 in Figs.11A and 11C, respectively) (curve 0 is the CV in the pH 11 buffer). The corresponding mass curves are plotted in Figs. 11B and 11D. Again, there is no oxidation of the alcohols by Ni(III), which again can be attributed to alcohol depletion at the interface due to its reaction with the gold substrate, since the current densities of peak P3 are a sizable fraction of those at the diffusion limit. In Figs. 11B and 11D the mass curves were also superimposed in region *d*, just after Ni(II) oxidation has been completed. Secondary alcohols barely affect the initial mass (Fig. 11B) in the pH 11 buffer (region *a)*, whereas 1-propanol does increase it (Fig. 11D). With the exception of 1-propanol, the mass changes in the Ni(III)/Ni(II) region are unaffected by the presence of the alcohols (regions *b*, *c* and *d* in Figs. 11B and 11D), as could be expected from the absence of change of peaks A1 and C1 in the CVs (Figs. 11A and 11C). Only in region *e*, in which the mass decreases markedly due to the reduction of gold oxide, is this mass decrease slightly lowered by the alcohols, probably because they decrease the amount of gold oxide by its chemical reaction with the alcohol.

Table 3. Peak current densities and peak potentials in the positive scan at 0.02 V s^{-1} of the peak of alcohol oxidation on different electrodes for 50 mM alcohols in the pH 11 buffer

	Alcohol Electrode	EG	1-propanol	2-propanol	ethanol
j_p mA cm^{-2}	Au/Q	0.64	0.33	0.33	0.12
	polyNiTSPc/Au/Q	1.40	0.99	0.58	0.35
	aged *polyNiTSPc*/Au/Q	0.43	0.24	0.26	0.14
E_p V vs. Ag/AgCl	Au/Q	0.43	0.36	0.33	0.35
	polyNiTSPc/Au/Q	0.48	0.37	0.36	0.43
	aged *polyNiTSPc*/Au/Q	0.43	0.35	0.31	0.37

The peak potentials and peak current densities in CVs at 0.02 V s^{-1} of the oxidation on the gold substrate of 50 mM ethylene glycol (EG), 1- and 2-propanol, and ethanol in the pH 11 buffer, at bare Au/Q electrodes, and at both freshly prepared and aged *polyNiTSPc*/Au/Q electrodes, are given in Table 3. Although alcohol oxidation takes place on the gold substrate, the film has a beneficial effect, since with it the peak current densities are 1.6-3.0 times those on Au/Q. However, ageing of the modified electrodes by RCVs at 0.01 V s^{-1} in 0.1 M NaOH decreases their activity, the peak current densities becoming even lower than those with Au/Q. A negative effect of ageing, attributed to the accumulation of adsorbed residues, has been reported previously for methanol oxidation at these electrodes [17]. The activity decrease of *polyNiTSPc* films for aliphatic, but not for aromatic, alcohols brought about by ageing indicate that oxidation residues remain adsorbed only on the former.

For aliphatic alcohols current saturation is reached at lower concentrations than for aromatic alcohols (not shown), in agreement with a low reaction rate. 1- and 2-propanol show very similar peak current densities, evidencing that the aldehyde is the only reaction product, the same occurring with 1- and 2-butanol.

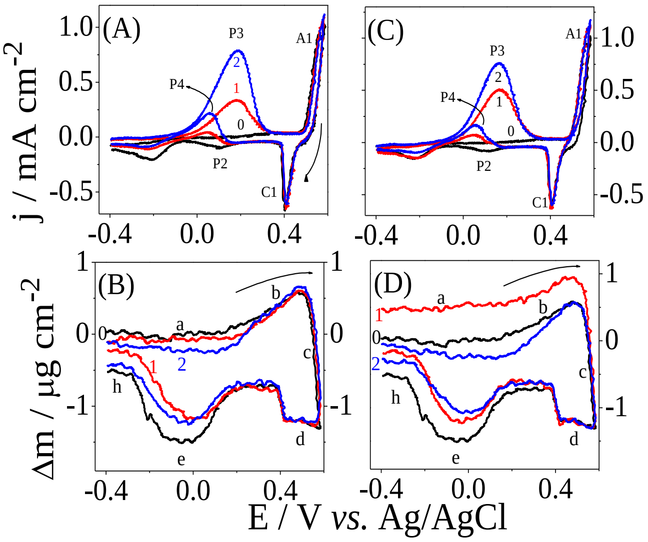

Figure 11. (A) and (C): CVs at 0.01 V s^{-1} of *polyNiTSPc*/Au/Q electrodes, and (B) and (D): the simultaneous recorded mass curves, in: pH 11 buffer (curve 0), in the presence of 20 mM 1-and 2-propanol (curves 1), and in the presence of 20 mM 1-and 2-butanol (curves 2). (A and B): secondary alcohols; (C and D): primary alcohols.

The butanols show higher current densities than the respective propanols, probably due to their incipient hydrophobic character, which can produce an increase of their concentration at the double layer. This effect is higher than with bare gold [5]. The current densities of aliphatic alcohols are smaller than those of BA, as occurs with gold electrodes [5], evidencing the importance of the hydrophobicity of the alcohol in its electrooxidation process, since on a hydrophobic surface hydrophobic molecules adsorb more than hydrophilic ones.

4. CONCLUSIONS

The aliphatic alcohols are oxidized on both $Ni(OH)_2$/GC-D and *polyNiTSPc*/GC-D. Remarkably, this is not so at all for BA: while it is easily oxidized on *polyNiTSPc*/GC-D, it is not oxidized at all on $Ni(OH)_2$/GC-D. We attribute this dramatic difference to hydrophobic-hydrophilic interactions: while the aromatic BA would easily adsorb on the phthalocyanine ring of *polyNiTSPc*, it would not do so on the highly hydrated $Ni(OH)_2$.

In the *CV* of the Au electrode coated with films of *polyNiTSPc* or $Ni(OH)_2$ the anodic peak of gold oxidation and the cathodic peak of gold oxide reduction continue appearing, which clearly shows that these films are very porous, allowing easy access of the electrolyte to the Au substrate. Due to this, the oxidation of *BA* at the very active Au substrate proceeds at so high a rate, and already at a potential lower than that of Ni(II) oxidation, that when Ni(III) is formed its reaction with *BA* proceeds at a much smaller rate than that of BA oxidation on Au. Obviously, when a GC substrate, which is completely inactive for the oxidation of aliphatic alcohols, is used, then these alcohols can be oxidized on a *polyNiTSPc* film by chemical reaction with Ni(III).

Although the previous *XPS* results indicated a very similar environment for the Ni(II) ion in *polyNiTSPc* and $Ni(OH)_2$ films, their electrochemical behaviour is different, which is probably associated with the hydrophobic-hydrophilic character of the film. The presence of a hydrophobic, freshly prepared *polyNiTSPc* film increases the oxidation current of aliphatic alcohols *on the gold substrate*, evidencing that the hydrophobic character of the film has a major importance in the oxidation of alcohols.

ACKNOWLEDGEMENTS
We are grateful to *DICYT-USACh* and *FONDECYT*-1070290 and -1100476 for financial support.

References

1. T. Iwasita, *Electrochim. Acta*, 47 (2002) 3663-3674
2. I. Sprague and P. Dutta, *Electrochim. Acta*, 56 (2011) 4518-4525
3. S-W Xie, S. Chen, Z-Q Liu and C-W Xu, *Int. J. Electrochem. Sci.*, 6 (2011) 882-888
4. A. Santasalo-Aarnio, Y. Kwon, E. Ahlberg, K. Kontturi, T. Kallio and M. T. M. Koper, *Electrochem. Comm.*, 13 (2011) 466-469
5. M. S. Ureta-Zañartu, C. Berríos, T. González, F. Fernández, D. Báez, R. Salazar and C. Gutiérrez, *Int. J. Electrochem. Sci.*, 7 (2012) xx-yy
6. R. B. Kutz, B. Braunschweig, P. Mukherjee, D. D. Dlott and A. Wieckowski, *J. Phys. Chem. Letters*, 2 (2011) 2236-2240
7. C. Berríos, J. F. Marco, C. Gutiérrez and M. S. Ureta-Zañartu, *J. Phys. Chem. B*, 112 (2008) 12644-12649
8. M. S. Ureta-Zañartu, A. Alarcón, C. Berrios, G. I. Cárdenas-Jirón, J. H. Zagal and C. Gutiérrez, *J. Electroanal. Chem.*, 580 (2005) 94-104
9. M. Wehrens-Dijksma and P. H. L. Notten, *Electrochim. Acta*, 51 (2006) 3609-3621
10. Z. Qi, H. Geng, X. Wang, C. Zhao, H. Ji, C. Zhang, J. Xu and Z. Zhang, *J. Power Sources*, 196 (2011) 5823-5828
11. F. Miao and B. Tao, *Electrochim. Acta*, 56 (2011) 6709-6714
12. A. J. Motheo, G. Tremiliosi-Filho, E. R. Gonzalez, K. B. Kokoh, J. M. Léger and C. Lamy, *J Appl. Electrochem.*, 36 (2006)1035-1041.
13. M. Jafarian, M. A. Haghighatbin, F. Gobal, M. G. Mahjani and S. Rayati, *J. Electroanal. Chem.*, 663 (2011) 1572-6657
14. C. Berríos, G. I. Cárdenas-Jirón; J. F. Marco, C. Gutiérrez and M. S. Ureta-Zañartu, *J. Phys. Chem.* A, 111 (2007) 2706-2714
15. C. Berríos, R. Arce, M. C. Rezende, M. S. Ureta-Zañartu and C. Gutiérrez, *Electrochim. Acta*, 53 (2008) 2768-2775
16. M. S. Ureta-Zañartu, A. Alarcón, G. Muñoz and C. Gutiérrez, *Electrochim. Acta*, 52 (2007) 7857-7864
17. F. Gobal, Y. Valadbeigi and L. M. Kasmaee, *J. Electroanal. Chem.*, 650 (2011) 219-225
18. S. Trevin, F. Bedioui, M. Villegas, G. Gómez and C. Bied-Charreton, *J. Mater. Chem.*, 7 (1997) 923-928

19. G. Roslonek and J. Taraszewska, *J. Electroanal. Chem*., 325(1992)285-300
20. A. Ciszewski and G. Milczarek, *J. Electroanal. Chem*., 413 (1996) 137-142
21. Y. Mo, E. Hwang and D. A. Scherson, *J. Electrochem. Soc*., 143 (1996) 37-43
22. M. Wehrens-Dijksma and P. H. L. Notten, *Electrochim. Acta*, 51(2006) 3609-3621
23. C-C Yang, *International J. Hydrogen Energy* 27(2002) 1071-1081
24. M. S. Ureta-Zañartu, C. Berríos, J. Pavez, J. Zagal, C. Gutiérrez and J. F. Marco, *J. Electroanal. Chem*., 553(2003) 147-156
25. F. Hahn, B. Beden, M. J. Croissant and C. Lamy, *Electrochim. Acta*, 31 (1986) 335-342
26. Y-C Weng and T-C Chou, *J. Electrochem. Soc*. 150 (2003) C385-C390
27. C. Berríos, M. S. Ureta-Zañartu and C. Gutiérrez, *Electrochim. Acta*, 53 (2007) 792-802
28. C. Berríos, J. F. Marco, C. Gutiérrez and M. S. Ureta-Zañartu, *Electrochim. Acta*, 54 (2009) 6417-6425
29. M. Fleichsmann, K. Korinek and D. Pletcher, *J. Electroanal. Chem.*, 31 (1971) 39-49
30. A. A. El-Shafei, *J. Electroanal. Chem*., 471 (1999) 89-95
31. I. Danae, M. Jafarian, F. Forouzandeh, F. Gobal and M.G. Mahjani, *Electrochim. Acta*, 53 (2008) 6602-6609
32. A. N. Golikand, M. Asgari, M. G. Maragheh and S. Shahrokhian, *J. Electroanal. Chem*. 588 (2006) 155-160
33. R. Ojani, J-B Raoof, S. Fathi and S. Alami-Valikchali, *J. Solid State Electrochem*., 15 (2011) 1935-1941
34. E. Antolini and E. R. Gonzalez, *J. Power Sources*, 195 (2010) 3431-3450
35. S. C. S. Lai, S. E. F. Kleijin, T.Z. Öztürk, V.C. van Rees Vellinga, J. Koning, P. Rodriguez and M. T. M. Koper, *Catalysis Today*, 154 (2010) 92-104.
36. P. Ocon, C. Alonso, R. Celdrán and J. González-Velasco, *J. Electroanal. Chem*. 206 (1986) 179-196